

36. A Domain Embedding Method for the Direct Numerical Simulation of Fluidization and Sedimentation Phenomena

R. Glowinski¹, T.-W. Pan², D.D. Joseph³

Introduction

Motivated by the *direct numerical simulation of particulate flow* (i.e., of the motion of fluid-particle mixtures) the authors of this paper, with the assistance of several collaborators, have introduced some years ago a computational methodology based on a *fictitious domain* formulation involving distributed Lagrange multipliers defined over the particles; this approach allows the flow computations to be done on a fixed space region of simple shape, giving thus to the practitioners the possibility of very fast solvers to treat, for example, the diffusion and the incompressibility if we assume that the fluid is viscous and incompressible. The above methodology will be briefly discussed in the next section and then applied to the direct simulations of the fluidization of 1204 identical rigid solid spherical particles contained in a “bed” of simple shape and of the sedimentation of 6400 disks in a 2D rectangular box. For more details on the methodology briefly discussed in this paper and for further numerical results obtained with it see [GHJ⁺97, GPH⁺98, PGH⁺98, GPHJ99, GPH⁺99, Pan99].

Mathematical Models for Particulate Flow: A Fictitious Domain Based Equivalent Formulation.

Modeling of the fluid-particle interaction.

Let $\Omega \subset \mathbb{R}^d (d = 2, 3)$ be a space region; we suppose that Ω is filled with an *incompressible viscous fluid* of density ρ_f and that it contains J moving rigid bodies P_1, P_2, \dots, P_J (see Figure 1 for a particular case where $d = 2$ and $J = 3$). We denote by \mathbf{n} the unit normal vector on the boundary of $\Omega \setminus \cup_{j=1}^J \overline{P}_j$, pointing outward to the flow region. Assuming that the only external force acting on the mixture is *gravity*, then, between *collisions* (assuming that collisions take place), the *fluid flow* is modeled by the following *Navier-Stokes equations*

¹Department of Mathematics, University of Houston, Houston, TX 77204-3476, roland@math.uh.edu

²Department of Mathematics, University of Houston, Houston, TX 77204-3476, pan@math.uh.edu

³Aerospace Engineering and Mechanics, University of Minneapolis, 107 Ackerman Hall, 110 Union Street, Minneapolis, MN 55455, joseph@aem.umn.edu

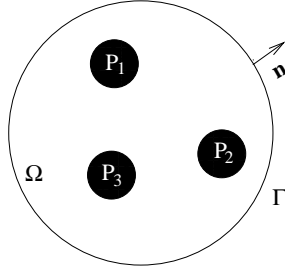


Figure 1: An example of two-dimensional flow region with three particles.

$$\begin{cases} \rho_f \left[\frac{\partial \mathbf{u}}{\partial t} + (\mathbf{u} \cdot \nabla) \mathbf{u} \right] = \rho_f \mathbf{g} + \nabla \cdot \boldsymbol{\sigma} \text{ in } \Omega \setminus \cup_{j=1}^J \overline{P_j(t)}, \\ \nabla \cdot \mathbf{u} = 0 \text{ in } \Omega \setminus \cup_{j=1}^J \overline{P_j(t)}, \\ \mathbf{u}(\mathbf{x}, 0) = \mathbf{u}_0(\mathbf{x}), \forall \mathbf{x} \in \Omega \setminus \cup_{j=1}^J \overline{P_j(0)}, \text{ with } \nabla \cdot \mathbf{u}_0 = 0, \end{cases} \quad (1)$$

to be completed by

$$\mathbf{u} = \mathbf{g}_0 \text{ on } \Gamma \text{ with } \int_{\Gamma} \mathbf{g}_0 \cdot \mathbf{n} d\Gamma = 0 \quad (2)$$

and by the following *no-slip boundary condition* on the boundary ∂P_j of P_j

$$\mathbf{u}(\mathbf{x}, t) = \mathbf{V}_j(t) + \boldsymbol{\omega}_j(t) \times \overline{\mathbf{G}_j(t)\mathbf{x}}, \quad \forall \mathbf{x} \in \partial P_j(t), \quad (3)$$

where, in (3), \mathbf{V}_j (resp., $\boldsymbol{\omega}_j$) denotes the *velocity of the center of mass* \mathbf{G}_j (resp., the *angular velocity*) of the j^{th} particle, for $j = 1, \dots, J$. In (1), the *stress-tensor* $\boldsymbol{\sigma}$ verifies

$$\boldsymbol{\sigma} = \boldsymbol{\tau} - p\mathbf{I}, \quad (4)$$

typical situations for $\boldsymbol{\tau}$ being

$$\begin{aligned} \boldsymbol{\tau} &= 2\nu\mathbf{D}(\mathbf{u}) = \nu(\nabla\mathbf{u} + \nabla\mathbf{u}^t) \text{ (Newtonian case),} \\ \boldsymbol{\tau} &\text{ is a nonlinear function of } \nabla\mathbf{u} \text{ (non - Newtonian case).} \end{aligned} \quad (5)$$

The motion of the particles is modeled by the following *Newton-Euler* equations

$$\begin{cases} M_j \frac{d\mathbf{V}_j}{dt} = M_j \mathbf{g} + \mathbf{F}_j, \\ \mathbf{I}_j \frac{d\boldsymbol{\omega}_j}{dt} + \boldsymbol{\omega}_j \times \mathbf{I}_j \boldsymbol{\omega}_j = \mathbf{T}_j, \end{cases} \quad (7)$$

for $j = 1, \dots, J$, where in (7):

- M_j is the *mass* of the j^{th} particle.
- \mathbf{I}_j is the *inertia tensor* of the j^{th} particle.

- \mathbf{F}_j is the resultant of the *hydrodynamical forces* acting on the j^{th} particle, i.e.

$$\mathbf{F}_j = (-1) \int_{\partial P_j} \boldsymbol{\sigma} \mathbf{nd}(\partial P_j). \quad (8)$$

- \mathbf{T}_j is the torque at \mathbf{G}_j of the hydrodynamical forces acting on the j^{th} particle, i.e.

$$\mathbf{T}_j = (-1) \int_{\partial P_j} \overrightarrow{\mathbf{G}_j \mathbf{x}} \times \boldsymbol{\sigma} \mathbf{nd}(\partial P_j). \quad (9)$$

- We have

$$\frac{d\mathbf{G}_j}{dt} = \mathbf{V}_j. \quad (10)$$

Equations (7) to (10) have to be completed by the following *initial conditions*:

$$P_j(0) = P_{0j}, \mathbf{G}_j(0) = \mathbf{G}_{0j}, \mathbf{V}_j(0) = \mathbf{V}_{0j}, \boldsymbol{\omega}_j(0) = \boldsymbol{\omega}_{0j}, \forall j = 1, \dots, J. \quad (11)$$

Remark 1 *If the flow-rigid body motion is two-dimensional, or if P_j is a spherical body made of an homogeneous material, then the nonlinear term $\boldsymbol{\omega}_j \times \mathbf{I}_j \boldsymbol{\omega}_j$ vanishes in (7).*

A global variational formulation of the fluid-particle interaction via the virtual power principle.

We suppose, in this section, that the fluid is *Newtonian* of viscosity ν . Let us denote by $P(t)$ the space region occupied at time t by the particles; we have thus $P(t) = \cup_{j=1}^J P_j(t)$. To obtain a *variational formulation* for the system of equations described as described above, we introduce the following *functional space* of *compatible test functions*:

$$\left\{ \begin{array}{l} W_0(t) = \{(\mathbf{v}, \mathbf{Y}, \boldsymbol{\theta}) \mid \mathbf{v} \in (H^1(\Omega \setminus \overline{P(t)}))^d, \mathbf{v} = \mathbf{0} \text{ on } \Gamma, \\ \mathbf{Y} = \{\mathbf{Y}_j\}_{j=1}^J, \boldsymbol{\theta} = \{\boldsymbol{\theta}_j\}_{j=1}^J, \text{ with } \mathbf{Y}_j \in \mathbb{R}^d, \boldsymbol{\theta}_j \in \mathbb{R}^3, \\ \mathbf{v}(\mathbf{x}, t) = \mathbf{Y}_j + \boldsymbol{\theta}_j \times \overrightarrow{\mathbf{G}_j(t) \mathbf{x}} \text{ on } \partial P_j(t), \forall j = 1, \dots, J\}; \end{array} \right. \quad (12)$$

in (12) we have $\boldsymbol{\theta}_j = \{0, 0, \theta_j\}$ if $d = 2$.

Applying the *virtual power principle* to the *whole* mixture (i.e., to the fluid *and* the particles) yields the following *global* variational formulation:

$$\left\{ \begin{array}{l} \rho_f \int_{\Omega \setminus \overline{P(t)}} \left[\frac{\partial \mathbf{u}}{\partial t} + (\mathbf{u} \cdot \nabla) \mathbf{u} \right] \cdot \mathbf{v} d\mathbf{x} + 2\nu \int_{\Omega \setminus \overline{P(t)}} \mathbf{D}(\mathbf{u}) : \mathbf{D}(\mathbf{v}) d\mathbf{x} \\ - \int_{\Omega \setminus \overline{P(t)}} p \nabla \cdot \mathbf{v} d\mathbf{x} + \sum_{j=1}^J M_j \dot{\mathbf{V}}_j \cdot \mathbf{Y}_j + \sum_{j=1}^J (\mathbf{I}_j \dot{\boldsymbol{\omega}}_j + \boldsymbol{\omega}_j \times \mathbf{I}_j \boldsymbol{\omega}_j) \cdot \boldsymbol{\theta}_j \\ = \rho_f \int_{\Omega \setminus \overline{P(t)}} \mathbf{g} \cdot \mathbf{v} d\mathbf{x} + \sum_{j=1}^J M_j \mathbf{g} \cdot \mathbf{Y}_j, \forall \{(\mathbf{v}, \mathbf{Y}, \boldsymbol{\theta}) \in W_0(t), \end{array} \right. \quad (13)$$

$$\int_{\Omega \setminus \overline{P(t)}} q \nabla \cdot \mathbf{u}(t) d\mathbf{x} = 0, \quad \forall q \in L^2(\Omega \setminus \overline{P(t)}), \quad (14)$$

$$\mathbf{u}(t) = \mathbf{g}_0(t) \text{ on } \Gamma, \quad (15)$$

$$\mathbf{u}(\mathbf{x}, t) = \mathbf{V}_j(t) + \boldsymbol{\omega}_j(t) \times \overrightarrow{\mathbf{G}_j(t)\mathbf{x}}, \quad \forall \mathbf{x} \in \partial P_j(t), \quad \forall j = 1, \dots, J, \quad (16)$$

$$\frac{d\mathbf{G}_j}{dt} = \mathbf{V}_j, \quad (17)$$

to be completed by the following *initial conditions*

$$\mathbf{u}(\mathbf{x}, 0) = \mathbf{u}_0(\mathbf{x}), \quad \forall \mathbf{x} \in \Omega \setminus \overline{P(0)}, \quad (18)$$

$$P_j(0) = P_{0j}, \quad \mathbf{G}_j(0) = \mathbf{G}_{0j}, \quad \mathbf{V}_j(0) = \mathbf{V}_{0j}, \quad \boldsymbol{\omega}_j(0) = \boldsymbol{\omega}_{0j}, \quad \forall j = 1, \dots, J. \quad (19)$$

In relations (13) to (19):

- We have denoted functions such as $\mathbf{x} \rightarrow \varphi(\mathbf{x}, t)$ by $\varphi(t)$.
- We have used the following notation

$$\begin{aligned} \mathbf{a} \cdot \mathbf{b} &= \sum_{k=1}^d a_k b_k, \quad \forall \mathbf{a} = \{a_k\}_{k=1}^d, \quad \mathbf{b} = \{b_k\}_{k=1}^d, \\ \mathbf{A} : \mathbf{B} &= \sum_{k=1}^d \sum_{l=1}^d a_{kl} b_{kl}, \quad \forall \mathbf{A} = (a_{kl})_{1 \leq k, l \leq d}, \quad \mathbf{B} = (b_{kl})_{1 \leq k, l \leq d}. \end{aligned}$$

- We have $\boldsymbol{\omega}_j(t) = \{0, 0, \omega_j(t)\}$ if $d = 2$.
- We assume that $\mathbf{u}(t) \in (H^1(\Omega \setminus \overline{P(t)}))^d$ and $p(t) \in L^2(\Omega \setminus \overline{P(t)})$.

A distributed Lagrange multiplier based fictitious domain method.

Following references [GHJ+97, GPH+98, PGH+98, GPHJ99, GPH+99, Pan99] we introduce the following variant of the virtual power formulation (13)-(19):

For a.e. $t > 0$, find $\mathbf{u}(t)$, $p(t)$, $\{\mathbf{V}_j(t), \mathbf{G}_j(t), \boldsymbol{\omega}_j(t)\}_{j=1}^J$, such that

$$\left\{ \begin{aligned} & \rho_f \int_{\Omega} \left[\frac{\partial \mathbf{u}}{\partial t} + (\mathbf{u} \cdot \nabla) \mathbf{u} \right] \cdot \mathbf{v} d\mathbf{x} - \int_{\Omega} p \nabla \cdot \mathbf{v} d\mathbf{x} + 2\nu \int_{\Omega} \mathbf{D}(\mathbf{u}) : \mathbf{D}(\mathbf{v}) d\mathbf{x} \\ & + \sum_{j=1}^J (1 - \rho_f / \rho_j) \left[M_j \frac{d\mathbf{V}_j}{dt} \cdot \mathbf{Y}_j + (\mathbf{I}_j \frac{d\boldsymbol{\omega}_j}{dt} + \boldsymbol{\omega}_j \times \mathbf{I}_j \boldsymbol{\omega}_j) \cdot \boldsymbol{\theta}_j \right] \\ & = \rho_f \int_{\Omega} \mathbf{g} \cdot \mathbf{v} d\mathbf{x} + \sum_{j=1}^J (1 - \rho_f / \rho_j) M_j \mathbf{g} \cdot \mathbf{Y}_j, \quad \forall \{\mathbf{v}, \mathbf{Y}, \boldsymbol{\theta}\} \in \tilde{W}_0(t), \end{aligned} \right. \quad (20)$$

$$\int_{\Omega} q \nabla \cdot \mathbf{u} d\mathbf{x} = 0, \quad \forall q \in L^2(\Omega), \quad (21)$$

$$\mathbf{u} = \mathbf{g}_0 \text{ on } \Gamma, \quad (22)$$

$$\mathbf{u}(\mathbf{x}, t) = \mathbf{V}_j(t) + \boldsymbol{\omega}_j(t) \times \overrightarrow{\mathbf{G}_j(t)\mathbf{x}}, \quad \forall \mathbf{x} \in P_j(t), \quad \forall j = 1, \dots, J, \quad (23)$$

$$\frac{d\mathbf{G}_j}{dt} = \mathbf{V}_j, \quad (24)$$

$$P_j(0) = P_{0j}, \quad \mathbf{V}_j(0) = \mathbf{V}_{0j}, \quad \boldsymbol{\omega}_j(0) = \boldsymbol{\omega}_{0j}, \quad \mathbf{G}_j(0) = \mathbf{G}_{0j}, \quad \forall j = 1, \dots, J, \quad (25)$$

$$\mathbf{u}(\mathbf{x}, 0) = \mathbf{u}_0(\mathbf{x}), \quad \forall \mathbf{x} \in \Omega \setminus \cup_{j=1}^J \overline{P_{0j}} \quad (26)$$

$$\mathbf{u}(\mathbf{x}, 0) = \mathbf{V}_{0j} + \boldsymbol{\omega}_{0j} \times \overrightarrow{\mathbf{G}_{0j}\mathbf{x}}, \quad \forall \mathbf{x} \in \overline{P_{0j}}, \quad \forall j = 1, \dots, J, \quad (27)$$

with, in relation (20), space $\tilde{W}_0(t)$ defined by

$$\tilde{W}_0(t) = \{(\mathbf{v}, \mathbf{Y}, \boldsymbol{\theta}) | \mathbf{v} \in (H_0^1(\Omega))^d, \mathbf{Y} = \{\mathbf{Y}_j\}_{j=1}^J, \boldsymbol{\theta} = \{\boldsymbol{\theta}_j\}_{j=1}^J, \text{ with } \mathbf{Y}_j \in \mathbb{R}^d, \boldsymbol{\theta}_j \in \mathbb{R}^3, \mathbf{v}(\mathbf{x}, t) = \mathbf{Y}_j + \boldsymbol{\theta}_j \times \overrightarrow{\mathbf{G}_j(t)\mathbf{x}} \text{ in } P_j(t), \forall j = 1, \dots, J\}.$$

In order to relax the *rigid body motion constraint* (23) we are going to employ a family $\{\boldsymbol{\lambda}_j\}_{j=1}^J$ of *Lagrange multipliers* so that $\boldsymbol{\lambda}_j(t) \in \Lambda_j(t)$ with

$$\Lambda_j(t) = (H^1(P_j(t)))^d, \forall j = 1, \dots, J. \tag{28}$$

We obtain, thus, the following *fictitious domain formulation with Lagrange multipliers*: For a.e. $t > 0$, find $\mathbf{u}(t)$, $p(t)$, $\{\mathbf{V}_j(t)$, $\mathbf{G}_j(t)$, $\boldsymbol{\omega}_j(t)$, $\boldsymbol{\lambda}_j(t)\}_{j=1}^J$, such that

$$\begin{cases} \mathbf{u}(t) \in (H^1(\Omega))^d, \mathbf{u}(t) = \mathbf{g}_0(t) \text{ on } \Gamma, p(t) \in L^2(\Omega), \\ \mathbf{V}_j(t) \in \mathbb{R}^d, \mathbf{G}_j(t) \in \mathbb{R}^d, \boldsymbol{\omega}_j(t) \in \mathbb{R}^3, \boldsymbol{\lambda}_j(t) \in \Lambda_j(t), \forall j = 1, \dots, J, \end{cases} \tag{29}$$

and

$$\begin{cases} \rho_f \int_{\Omega} \left[\frac{\partial \mathbf{u}}{\partial t} + (\mathbf{u} \cdot \nabla) \mathbf{u} \right] \cdot \mathbf{v} dx - \int_{\Omega} p \nabla \cdot \mathbf{v} dx \\ + 2\nu \int_{\Omega} \mathbf{D}(\mathbf{u}) : \mathbf{D}(\mathbf{v}) dx + \sum_{j=1}^J (1 - \rho_f/\rho_j) M_j \frac{d\mathbf{V}_j}{dt} \cdot \mathbf{Y}_j \\ + \sum_{j=1}^J (1 - \rho_f/\rho_j) (\mathbf{I}_j \frac{d\boldsymbol{\omega}_j}{dt} + \boldsymbol{\omega}_j \times \mathbf{I}_j \boldsymbol{\omega}_j) \cdot \boldsymbol{\theta}_j \\ - \sum_{j=1}^J \langle \boldsymbol{\lambda}_j, \mathbf{v} - \mathbf{Y}_j - \boldsymbol{\theta}_j \times \overrightarrow{\mathbf{G}_j \mathbf{x}} \rangle_j \\ = \rho_f \int_{\Omega} \mathbf{g} \cdot \mathbf{v} dx + \sum_{j=1}^J (1 - \rho_f/\rho_j) M_j \mathbf{g} \cdot \mathbf{Y}_j, \\ \forall \mathbf{v} \in (H_0^1(\Omega))^d, \forall \mathbf{Y}_j \in \mathbb{R}^d, \forall \boldsymbol{\theta}_j \in \mathbb{R}^3, \end{cases} \tag{30}$$

$$\langle \boldsymbol{\mu}_j, \mathbf{u}(t) - \mathbf{V}_j(t) - \boldsymbol{\omega}_j(t) \times \overrightarrow{\mathbf{G}_j(t)\mathbf{x}} \rangle_j = 0, \forall \boldsymbol{\mu}_j \in \Lambda_j(t), \forall j = 1, \dots, J, \tag{31}$$

completed by relations (21), (24)-(27). The two most natural choices for $\langle \cdot, \cdot \rangle_j$ are defined by

$$\langle \boldsymbol{\mu}, \mathbf{v} \rangle_j = \int_{P_j(t)} (\boldsymbol{\mu} \cdot \mathbf{v} + \delta_j^2 \nabla \boldsymbol{\mu} : \nabla \mathbf{v}) dx, \forall \boldsymbol{\mu} \text{ and } \mathbf{v} \in \Lambda_j(t), \tag{32}$$

$$\langle \boldsymbol{\mu}, \mathbf{v} \rangle_j = \int_{P_j(t)} (\boldsymbol{\mu} \cdot \mathbf{v} + \delta_j^2 \mathbf{D}(\boldsymbol{\mu}) : \mathbf{D}(\mathbf{v})) dx, \forall \boldsymbol{\mu} \text{ and } \mathbf{v} \in \Lambda_j(t), \tag{33}$$

with δ_j a *characteristic length* (the diameter of P_j , for example). Other choices are possible as shown in, e.g, ref. [GPHJ99].

On the discretization of problem (29)-(31).

The *space approximation* (resp., *time discretization*) of problem (29)-(31) by *finite element method* (resp., *operator splitting*) methods is discussed in refs. [GHJ+97, GPJ+98, PGH+98, GPHJ99, GPH+99, Pan99]; the above references also include a discussion of the numerical treatment of *particle/particle* and *particle/boundary collisions*.

Numerical Simulations

The Fluidization of a Bed of 1204 Particles.

We consider here the simulation of the *fluidization* in a bed of 1,204 spherical particles. The computational domain is $\Omega = (0, 0.6858) \times (0, 20.3997) \times (0, 44.577)$. The thickness of this bed is slightly larger than the diameter of the particles which is $d = 0.635$, so there is only one layer of balls in the $0x_2$ direction (the above lengths are in centimeters). In [FJL87] many experimental results related to this type of “almost two-dimensional” beds are presented. The fluid is incompressible, viscous, and Newtonian; its density is $\rho_f = 1$ and its viscosity is $\nu_f = 10^{-2}$. We suppose that at $t = 0$ the fluid and the particles are at rest. The boundary condition for the velocity field is

$$\mathbf{u}(t) = \begin{cases} \mathbf{0} & \text{on the four vertical walls,} \\ 5 \begin{pmatrix} 0 \\ 0 \\ 1 - e^{-50t} \end{pmatrix} & \text{on the two horizontal walls.} \end{cases}$$

The density of the balls is $\rho_s = 1.14$. We suppose that the fluid can enter and leave the bed. The mesh size for the velocity field is $h_\Omega = 0.06858$ (corresponding to 2×10^6 vertices for the velocity mesh), while it is $h_p = 2h_\Omega$ for the pressure (corresponding to 2.9×10^5 vertices for the pressure mesh). The time step is $\Delta t = 10^{-3}$. The initial position of the balls is shown in Figure 2. After starting pushing the balls up, we observe that the inflow creates cavities propagating among the balls in the bed. Since the inflow velocity is much higher than the critical fluidization velocity (of the order of 2.5 here), many balls are pushed directly to the top of the bed. Those balls at the top of the bed are stable and closely packed while the others are circling around at the bottom of the bed. Those numerical results are very close to experimental ones obtained at the University of Minnesota and have been visualized in Figures 2 and 3 (where the lengths are in inches this time). In the simulation, the maximum particle Reynolds number is 1,512 while the maximum averaged particle Reynolds number is 285. The computations were done on an *SGI Origin 2000*, using a partially parallelized code; the computational time is approximately 110 sec./time step.

Sedimentation of 6,400 circular particles in a two-dimensional cavity. Rayleigh-Taylor instability for particulate flow.

The test problem that we consider now concerns the simulation of the motion of 6,400 sedimenting circular disks in the closed cavity $\Omega = (0, 8) \times (0, 12)$. The diameter d of the disks is $1/12$ and the position of the disks at time $t = 0$ is shown in Figure 4. The solid fraction in this test case is 34.9%. The disks and the fluid are at rest a time $t = 0$. The density of the fluid is $\rho_f = 1$ and the density of the disks is $\rho_s = 1.1$. The viscosity of the fluid is $\nu_f = 10^{-2}$. The time step is 10^{-3} . The mesh size for the velocity field is $h_\Omega = 1/192$ (the velocity triangulation has thus about 3.5×10^6 vertices) while the pressure mesh size is $h_p = 2h_\Omega$ implying, approximately, 885,000 vertices for the pressure triangulation. For this test problem where many particles “move around” a fine mesh is required essentially everywhere. The computational time per time step

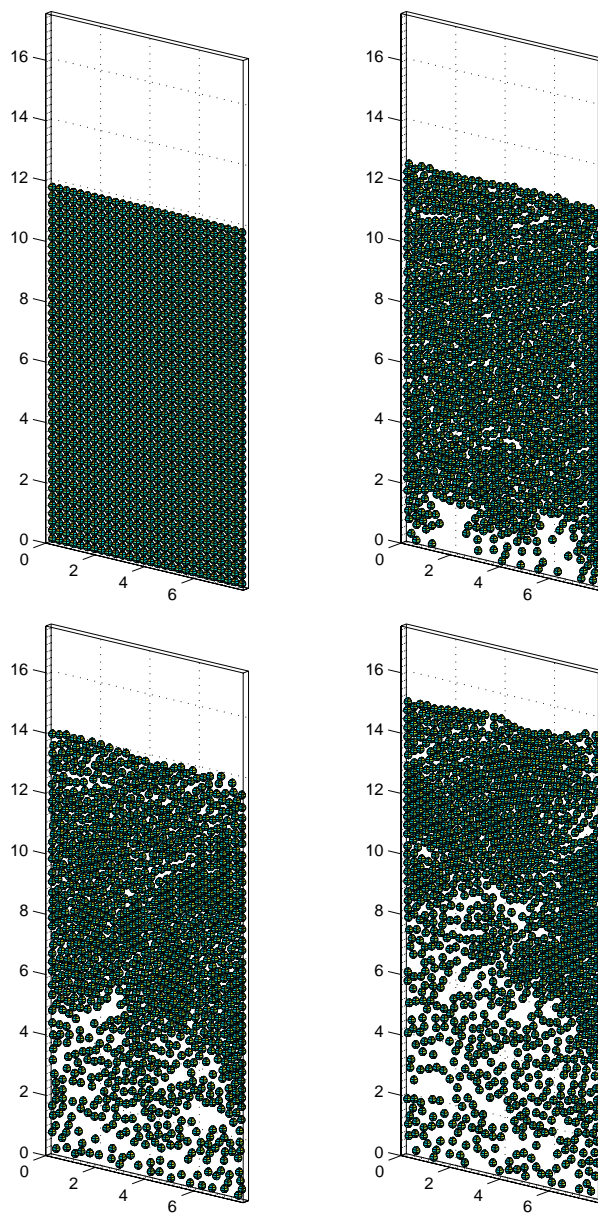


Figure 2: Fluidization of 1,204 spherical particles: positions of the particles at $t = 0$, 1.5, $t = 3$ and 4.5 (from left to right and from top to bottom).

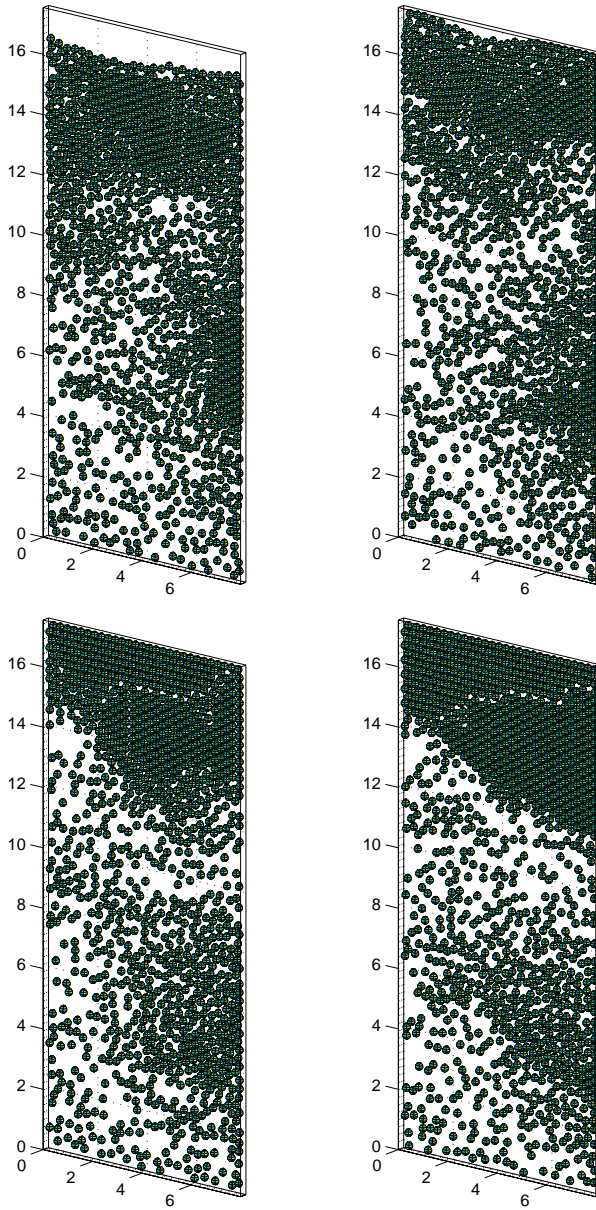


Figure 3: Fluidization of 1,204 spherical particles: positions of the particles at $t = 6$, 7, 8 and 10 (from left to right and from top to bottom).

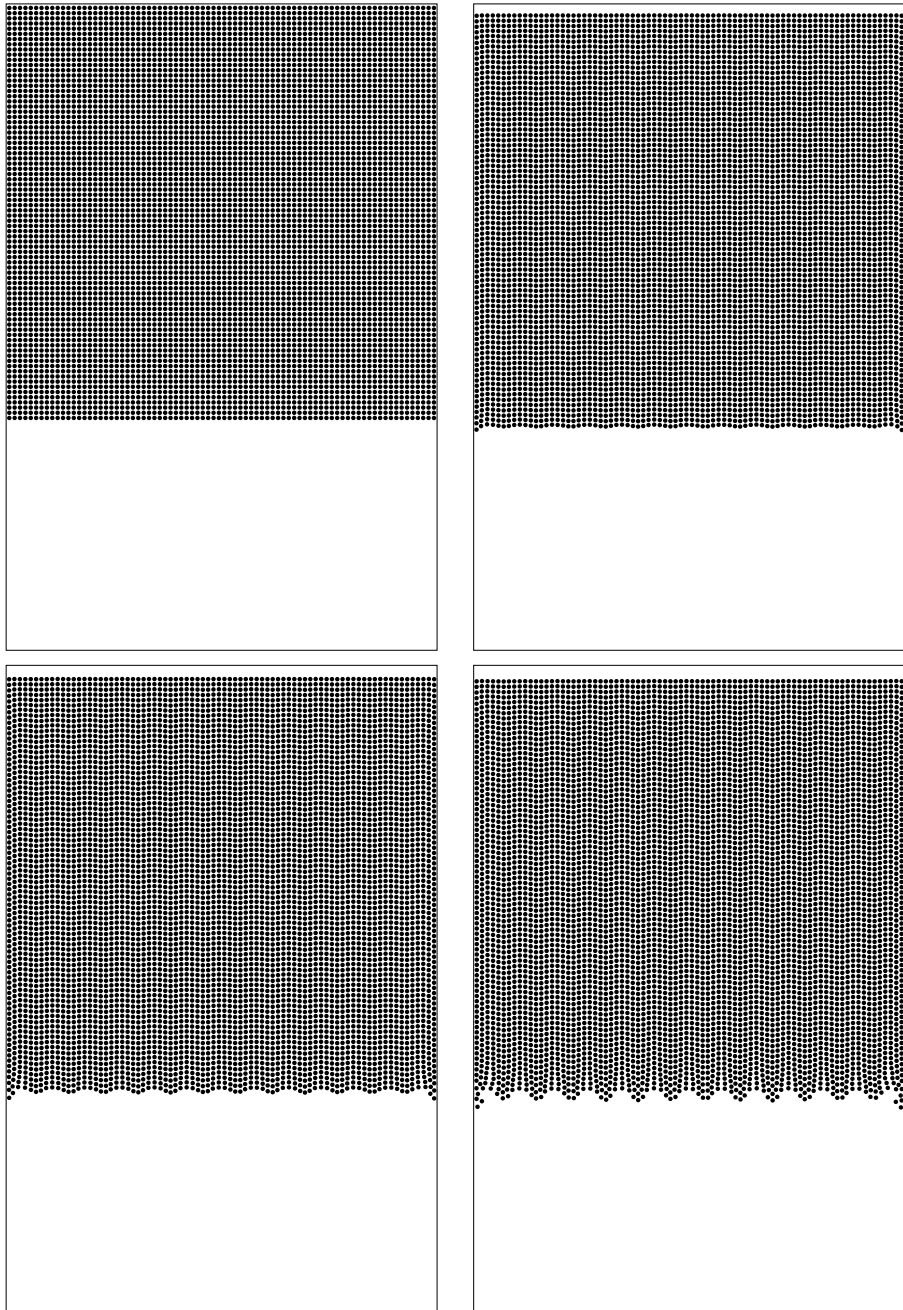


Figure 4: Sedimentation of 6,400 particles: positions at $t = 0, 0.4, 0.5, 0.6$ (from left to right and from top to bottom), and visualization of the Rayleigh-Taylor instability.

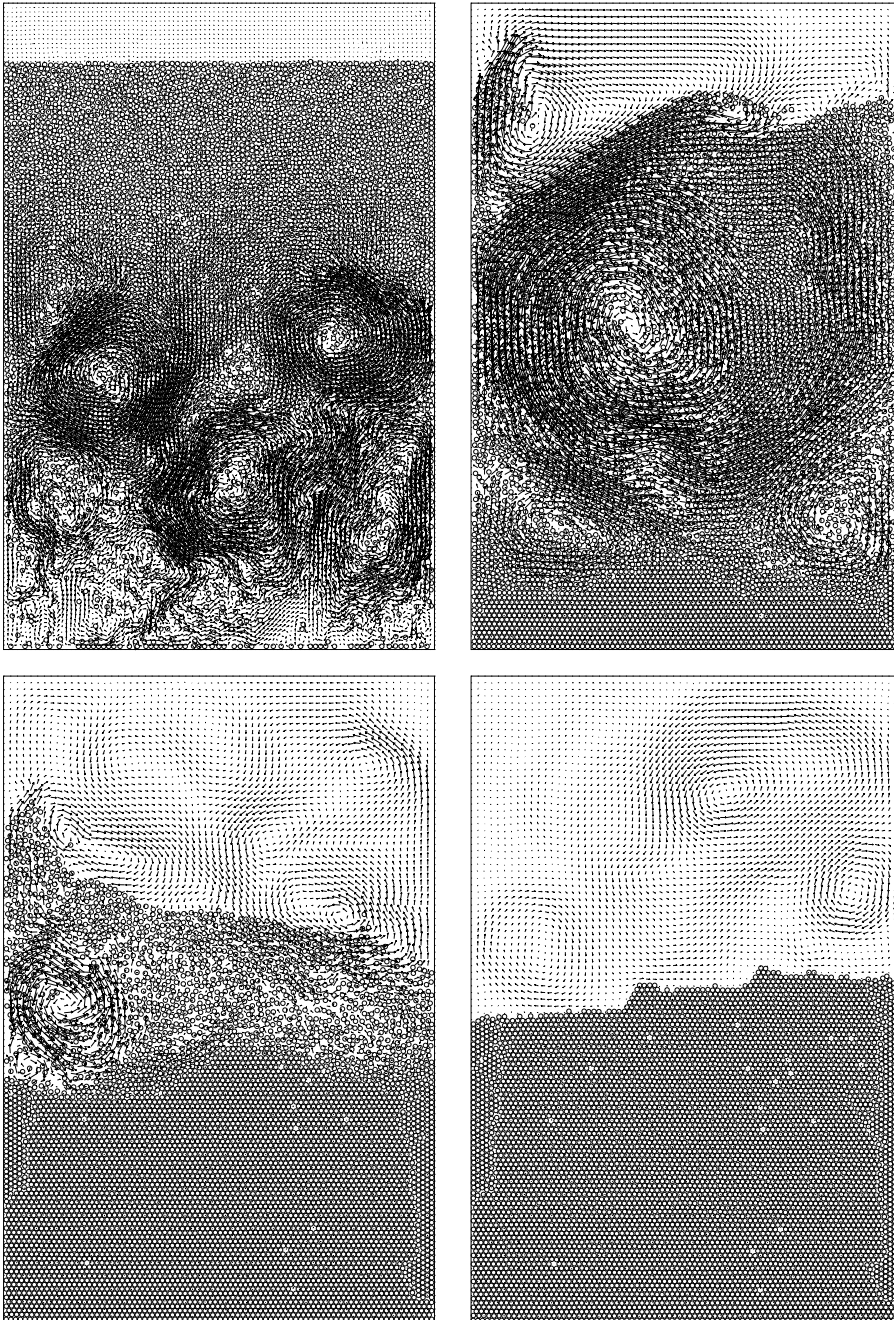


Figure 5: Sedimentation of 6,400 particles: positions at $t = 2.6, 5, 9, 13$ (from left to right and from top to bottom), and visualization of the Rayleigh-Taylor instability.

is approximately 10 min. on a *DEC Alpha 500-au* workstation, implying that to simulate *one time unit* of the phenomenon under consideration *we need, practically, a full week*. The evolution of the 6,400 disks sedimenting in Ω is shown in Figures 4 and 5. The maximum particle Reynolds number in the entire evolution is 72.64. Figure 4 clearly shows the development of a "text-book" *Rayleigh-Taylor instability*. This instability develops into a fingering phenomenon and many symmetry breaking and other bifurcation phenomena, including drafting, kissing and tumbling, take place at various scales and times; similarly vortices of various scales develop and for a while the phenomenon is clearly chaotic, which is not surprising after all for a 6,400-body problem. Finally, the particles settle at the bottom of the cavity and the fluid returns to rest.

Acknowledgments

We acknowledge the helpful comments and suggestions of E. J. Dean, V. Girault, J. He, T.I. Hesla, Y. Kuznetsov, J. Periaux, G. Rodin, A. Sameh, V. Sarin, and P. Singh, and also the support of the Supercomputing Institute at the University of Minnesota concerning the use of an SGI Origin2000. We acknowledge also the support of the NSF (Grants ECS-9527123, CTS-9873236, and DMS-9973318) and Dassault Aviation.

References

- [FJL87]A. F. Fortes, D. D. Joseph, and T. S. Lundgren. Nonlinear mechanics of fluidization of beds of spherical particles. *J. Fluid Mech.*, 177:467–483, 1987.
- [GHJ+97]R. Glowinski, T. I. Hesla, D.D. Joseph, T.W. Pan, and J. Periaux. Distributed Lagrange multiplier methods for particulate flows. In M.O. Bristeau, G.J. Etgen, W. Fitzgibbon, J.L. Lions, J. Periaux, and M.F. Wheeler, editors, *Computational Science for the 21st Century*, pages 270–279, Chichester, 1997. Wiley.
- [GPH+98]R. Glowinski, T.W. Pan, T.I. Hesla, D.D. Joseph, and J. Periaux. A fictitious domain method with distributed Lagrange multipliers for the numerical simulation of particulate flow. In J. Mandel, C. Farhat, , and X.C. Cai, editors, *Domain Decomposition Methods 10*, pages 121–137, Providence, RI, 1998. AMS.
- [GPH+99]R. Glowinski, T. W. Pan, T. I. Hesla, D. D. Joseph, and J. Periaux. A distributed Lagrange multiplier/fictitious domain method for flows around moving rigid bodies: Application to particulate flow. *Int. J. Numer. Meth. Fluids*, 30:1043–1066, 1999.
- [GPHJ99]R. Glowinski, T.W. Pan, T.I. Hesla, and D.D. Joseph. A distributed Lagrange multiplier/fictitious domain method for particulate flow. *International Journal of Multiphase Flow*, 25:755–794, 1999.
- [Pan99]T. W. Pan. Numerical simulation of the motion of a ball falling in an incompressible viscous fluid. *C. R. Acad. Sci. Paris*, 327, Série 2, b:1035–1038, 1999.
- [PGH+98]T. W. Pan, R. Glowinski, T. I. Hesla, D. D. Joseph, and J. Periaux. Numerical simulation of the Rayleigh-Taylor instability for particulate flow. In M. Hafez and J. C. Heinrich, editors, *Proceedings of the Tenth International Conference on Finite Elements in Fluids*, pages 217–222, 1998.

